AN EFFECTIVE TECHNIQUE FOR REDUCING THE TRUNCATION ERROR IN THE NEAR-FIELD-FAR-FIELD TRANSFORMATION WITH PLANE-POLAR SCANNING

F. D'Agostino, F. Ferrara, C. Gennarelli, R. Guerriero and G. Riccio

Dipartimento di Ingegneria dell'Informazione ed Ingegneria Elettrica
University of Salerno
Via Ponte Don Melillo, 84084 Fisciano (Salerno), Italy

Abstract—An effective approach is proposed in this paper for estimating the near-field data external to the measurement region in the plane-polar scanning. It relies on the nonredundant sampling representations of the electromagnetic field and makes use of the singular value decomposition method for the extrapolation of the outside samples. It is so possible to reduce in a significant way the error due to the truncation of the measurement zone thus increasing the far-field angular region of good reconstruction. The comparison of such an approach, based on the optimal sampling interpolation expansions, with an existing procedure using the cardinal series has highlighted that the proposed technique works better. Some numerical tests are reported for demonstrating its effectiveness.

1. INTRODUCTION

The nonredundant sampling representations of electromagnetic (EM) fields [1], which are based on the spatial bandlimitation properties [2] of the fields radiated by finite size sources, allow a very remarkable reduction of the near-field (NF) data to be acquired in the case of electrically large antennas and extended scanning regions. As a matter of fact, the NF data required to perform the near-field-far-field (NF-FF) transformations are recovered from the collected ones by using proper sampling interpolation formulas [3–10].

When the measurement region is truncated, such as in the cylindrical and planar scannings, an inevitable truncation error affects the NF data reconstruction in the zones close to the boundary of such

a region. As a consequence, the reconstruction results to be accurate in a zone smaller than the measurement one (since the required guard samples must belong to this last) and this implies a reduction of the angular region wherein an accurate FF reconstruction is attained. Of course, an enlargement of this last region can be obtained by decreasing the distance between the antenna under test (AUT) and the scanning surface. However, such a distance cannot be reduced beyond certain limits, otherwise the interactions between the AUT and the probe cannot be neglected any more.

An extension of the zone of "good NF reconstruction" is achievable by employing the optimal sampling interpolation (OSI) expansions instead of the cardinal series (CS) ones. In fact, when evaluating the field (or the voltage measured by the probe) at each needed point, these last require the use of many samples to keep the truncation error low and this leads to a large computational time too. On the contrary, the OSI expansions minimize the truncation error for a given number of retained samples and, therefore, they require only a reduced number of data in the neighbourhood of the output point. Furthermore, the use of OSI expansions allows one to overcome the other serious drawback of the CS ones, i.e., the propagation of the errors affecting the data from high to low field (voltage) regions [11], due to the slow decay of the interpolation functions.

It is worth noting that, although the use of the nonredundant sampling representations of the EM field is extremely convenient from the data reduction viewpoint, it gives rise to an unavoidable decrease in the ratio between the extensions of the accurate reconstruction zone and the measurement one. In fact, in such a case the guard samples represent a more relevant percentage of the overall number of data and lie in the peripheral zones, where the sample spacing is remarkably greater than in the central region. Accordingly, in order to obtain an accurate field (voltage) reconstruction in the whole measurement region, it becomes very important to estimate a proper number of outside samples.

In light of the above discussion, we are led to the following extrapolation problem: estimation of a (spatially) bandlimited function outside the observation region from the knowledge of its internal samples taken at a rate greater than the Nyquist one. As well-known, this is an ill-posed problem widely studied in literature with reference to the case of bandlimited signals which are known only in a finite time interval [12–21].

It is well-known that a continuous bandlimited signal can be extrapolated, without error, outside any finite interval. To this end, a Taylor series expansion can be used, since such a signal is analytic.

In practice, such a procedure is not feasible, because observed data are always corrupted by noise and the evaluation of derivatives is a noise-sensitive process. A different procedure using the prolate spheroidal wave functions has been proposed by Slepian and Pollak in [12]. Unfortunately, also this method is sensitive to the errors affecting the data and is onerous from the computational viewpoint. Papoulis introduced in [13] an iterative algorithm, which reduces at each iteration the mean-square error between the estimated and the original (time unbounded) signal. He compared it with that using the prolate spheroidal wave functions and showed that his method works better.

When considering discrete signals, the analyticity property vanishes, due to their sampling representation. Therefore, other constraints besides the limited bandwidth assumption are required in order to achieve an accurate solution. A discrete version of the iterative algorithm proposed by Papoulis has been developed in [14]. Moreover, in the same paper, a noniterative method has been proposed for solving the extrapolation problem from noise-free observations by means of an extrapolation matrix. In [15], Cadzow proposed a different extrapolation matrix, which does not have the existence problem of that suggested in [14]. In both papers, the solutions for the discrete case have been obtained by sampling the continuous solutions. The criterion of the minimum norm least squares for the extrapolation of the signal from observations containing additive noise has been introduced by Jain and Ranganath in [16]. In any case, as explicitly stated in [17], extrapolation techniques in presence of noise must be used judiciously in order to obtain reasonable results. Since the extrapolation can be viewed as a minimum norm least squares solution of a generally ill-posed system of linear equations, Sullivan and Liu suggested the use of the singular value decomposition (SVD) method for controlling the ill-conditioning [18]. A regularization procedure, based on the SVD and employing multiple regularization parameters to be determined optimally, has been proposed in [19] to deal with data affected by white Gaussian noise. Other considerations on the stability of the estimation procedure can be found in [20].

As explicitly stated in [21], when the samples are error affected, an accurate extrapolation of the signal is possible for at most a bounded distance beyond the observation interval. Accordingly, since physical measurements can never be perfect, this implies that only few samples external to the observation interval can be reliably estimated. This last consideration justifies why the extrapolation techniques have scarcely attracted the attention of the antenna measurement community. In fact, until the standard and redundant sampling representations (based

on the truncation of the spectrum to the visible region and, then, using a sample spacing at most equal to $\lambda/2$, λ being the wavelength) were the only available ones, the estimation of few external samples would have allowed a very limited extension of the zone wherein the near field was known.

The development of nonredundant sampling representations of EM fields has deeply modified the scenario [22]. In fact, by using these last representations, the sample spacing, as already stated, increases remarkably when moving far away from the center of the scanning region. Accordingly, even the estimation of very few samples external to such a region allows a noticeable extension of the zone wherein the near field is known, thus enlarging in a significant way the angular region wherein an accurate FF reconstruction is attained. In this framework, an approach for reducing the truncation error in the NF-FF transformations with plane-polar and cylindrical scannings has been developed in [22, 23] and [24], respectively. Such an approach is based on the aforementioned nonredundant representations and makes use of the CS expansions and of the SVD method for recovering the outside data.

A convenient OSI based extrapolation procedure for estimating the outside samples on a NF line is described in the following Section and compared with the technique using the CS expansions. Such an approach is properly extended in Section 3 to the extrapolation of the NF data external to the measurement region in the plane-polar scanning. At last, conclusions are collected in Section 4.

2. NF EXTRAPOLATION ALONG A LINE

In this Section the OSI expansions based extrapolation technique for recovering the samples external to the measurement region along a straight line in the NF region of an electrically large antenna is described and compared with that employing the CS expansions. Quite analogous results can be obtained when considering a two-dimensional observation domain too.

Without any loss of generality, let us consider an AUT enclosed in an oblate ellipsoidal surface Σ (having major and minor semi-axes equal to a and b) and a radial line of a plane-polar domain at distance d in the NF region (see Fig. 1).

According to [1], a nonredundant sampling representation can be obtained by introducing the "reduced electric field"

$$\underline{F}(\xi) = \underline{E}(\xi)e^{j\gamma(\xi)} \tag{1}$$

wherein the phase factor γ to be singled out from the field expression
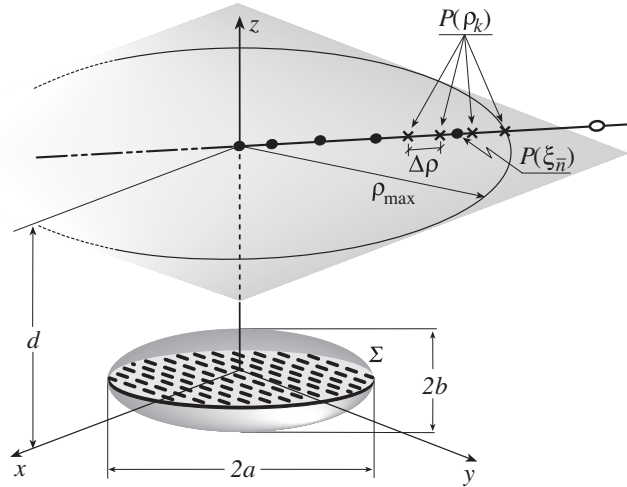
Figure 1. Relevant to a rectilinear observation domain. Dots: regular samples. Crosses: extra samples.

and the optimal parameter ξ for describing the radial line are given by

$$\gamma = \beta a \left[v\sqrt{\frac{(v^2 - 1)}{(v^2 - \varepsilon^2)}} - \mathrm{E}\left(\cos^{-1}\sqrt{\frac{(1 - \varepsilon^2)}{(v^2 - \varepsilon^2)}}\Big|\varepsilon^2 \right) \right] \qquad (2)$$

$$\xi = \frac{\pi}{2}\mathrm{E}\left(\sin^{-1} u|\varepsilon^2 \right) / \mathrm{E}(\pi/2|\varepsilon^2) \qquad (3)$$

In the above relations, β is the wavenumber, $\varepsilon = f/a$ is the eccentricity of the spheroid, $2f$ is its focal distance, $\mathrm{E}(\cdot|\cdot)$ is the elliptic integral of second kind, and $u = (r_1 - r_2)/2f$, $v = (r_1 + r_2)/2a$ are the elliptic coordinates, $r_{1,2}$ being the distances from the observation point P to the foci.

The reduced field is characterized by a spatial bandwidth $W_\xi = \beta\ell'/2\pi$ (ℓ' being the length of the ellipse intersection curve between the meridian plane through the radial line and Σ), and its value can be evaluated at any point on the radial line at φ via the following OSI expansion [1]:

$$\underline{F}(\xi,\varphi) = \sum_{n=n_0-q+1}^{n_0+q} \underline{F}(\xi_n,\varphi)\Omega_N(\xi - \xi_n)D_{N''}(\xi - \xi_n) \qquad (4)$$

where $\underline{F}(\xi_n,\varphi)$ are the reduced field samples, $n_0 = \mathrm{Int}\,(\xi/\Delta\xi)$ is the index of the sample nearest (on the left) to P, $2q$ is the number of

retained samples, Int (x) gives the integer part of x, and

$$\xi_n = n\Delta\xi = 2\pi n/(2N'' + 1); \quad N'' = \text{Int}(\chi N') + 1 \qquad (5)$$
$$N' = \text{Int}(\chi' W_\xi) + 1; \qquad\qquad N = N'' - N' \qquad (6)$$

$\chi' > 1$ and $\chi > 1$ being the bandwidth enlargement and oversampling factors, which allow to control the bandlimitation and truncation errors, respectively. Moreover,

$$D_{N''}(\xi) = \frac{\sin[(2N'' + 1)\xi/2]}{(2N'' + 1)\sin(\xi/2)} \qquad (7)$$

$$\Omega_N(\xi) = \frac{T_N[2(\cos(\xi/2)/\cos(\xi_0/2))^2 - 1]}{T_N[2/\cos^2(\xi_0/2) - 1]} \qquad (8)$$

are the Dirichlet and Tschebyscheff Sampling functions, wherein $T_N(\cdot)$ is the Tschebyscheff polynomial of degree N and $\xi_0 = q\Delta\xi$.

Since the linear sample spacing along the radial line increases remarkably when moving far away from the origin, it is expected that, when extended measurement regions are considered, even the estimation of very few outside data enlarges significantly the zone wherein the near field is known.

Let us now tackle the problem of estimating the NF samples external to the measurement interval $[-\rho_{\max}, \rho_{\max}]$ on the considered radial line at φ (see Fig. 1). In order to explain the methodology, let us consider the right-hand side of the interval of interest. If $\overline{q} \leq q$ is the number of the external samples to be estimated, let us assume the knowledge of the field components at the $K \geq \overline{q}$ extra points $P(\rho_k, \varphi)$, spaced at fixed step $\Delta\rho$ from the end. Then, for each of these points, just $\overline{q}$ unknown outside samples are always involved in the OSI expansion (4). Accordingly, for each reduced field component F, we have:

$$\sum_{n=\overline{n}+1}^{\overline{n}+\overline{q}} F(\xi_n, \varphi)\Omega_N(\xi(\rho_k) - \xi_n)D_{N''}(\xi(\rho_k) - \xi_n) = F(\xi(\rho_k), \varphi) +$$

$$- \sum_{n=n_0-q+1}^{\overline{n}} F(\xi_n, \varphi)\Omega_N(\xi(\rho_k) - \xi_n)D_{N''}(\xi(\rho_k) - \xi_n) = b_k, \ k = 1, \dots, K$$

$$(9)$$

where $\overline{n}$ is the index of the last "regular sample" inside $[0, \rho_{\max}]$, and it is assumed that $\overline{n} + \overline{q} \leq n_0 + q$.

These K equations can be rewritten in matrix form as

$$\underline{\underline{A}}\,\underline{x} = \underline{b} \qquad (10)$$

where $\underline{b}$ is the sequence of the known terms, $\underline{x}$ is the sequence of the unknown outside samples $F(\xi_n, \varphi)$, with $n = \overline{n} + 1, \ldots, \overline{n} + \overline{q}$, and $\underline{\underline{A}}$ is the $K \times \overline{q}$ matrix, whose elements are given by the weight functions in the considered OSI expansion:

$$A_{kn} = \Omega_N(\xi(\rho_k) - \xi_n)D_{N''}(\xi(\rho_k) - \xi_n) \tag{11}$$

As already stated, the overdetermined linear system (10) is ill-conditioned due to the presence of the bandlimitation and measurement errors. As a consequence, the vector of the known terms generally does not belong to the range of $\underline{A}$, i.e., the subspace spanned by such a matrix. As well-known [25, 26], a convenient technique to handle this problem and to find a solution, which is the best approximation in the least squares sense of the system (10), is obtained by using the SVD.

The approach proposed in [22] makes use of the CS expansion for the field interpolation instead of the OSI one. According to such an interpolation scheme, a reduced field component at the point $P(\xi, \varphi)$ can represented by the following expansion:

$$F(\xi, \varphi) = \sum_{m=-M}^{M} F(\xi_m, \varphi) \operatorname{sinc}\left[\chi' W_\xi(\xi - \xi_m)\right] \tag{12}$$

where $\operatorname{sinc}(\xi)$ is the $\sin(\xi)/\xi$ function,

$$\xi_m = m\Delta\xi = m\pi/(\chi' W_\xi); \qquad M = \operatorname{Int}(\chi' W_\xi/2] \tag{13}$$

It is worthy to note that the number of samples in the whole unbounded observation line is $2M + 1$, whereas the number of samples falling in the finite measurement interval $[-\rho_{\max}, \rho_{\max}]$ is $2\overline{m} + 1$, with $\overline{m} = \operatorname{Int}(\xi(\rho_{\max})/\Delta\xi)$.

Expansion (12) is employed to reconstruct the field components at each extra sampling point, thus getting overdetermined linear systems, which can be solved by using the SVD method. Two different extrapolation procedures have been proposed in [22] for estimating the outside samples. In the former, all the "regular samples" are unknown (both the samples external to the measurement interval and those falling inside it), and the extra samples are obtained by oversampling the field at points which are uniformly spaced in ρ. Such an approach allows the filtering of part of the noise affecting the measured data and falling outside the AUT spatial bandwidth. However, it becomes very onerous from the computational viewpoint in the here considered case of electrically large antennas and extended scanning regions. Therefore, it will not be considered in the following.

In the latter, only the regular samples external to the measurement interval are considered as unknowns and the "extra samples" $F(\tilde{\xi}_k, \varphi)$ are collected, starting from the boundary of the considered interval, at the middle points (in ξ) between two consecutive regular samples. Since only a small number of outside samples can reliably recovered, it is convenient to reduce the number of unknowns, cutting away those corresponding to the farther sampling points. Moreover, a number of extra samples less than twice the number of unknowns is considered in order to reduce the ill-conditioning of the problem [22].

In light of the above discussion, by considering the right-hand side of the interval of interest, we get the following overdetermined linear system:

$$\sum_{m=\overline{m}+1}^{\overline{m}+\overline{q}} F(\xi_m, \varphi) \operatorname{sinc}\left[\chi' W_\xi(\tilde{\xi}_k - \xi_m)\right] = F(\tilde{\xi}_k, \varphi) +$$

$$- \sum_{m=-\overline{m}}^{\overline{m}} F(\xi_m, \varphi) \operatorname{sinc}\left[\chi' W_\xi(\tilde{\xi}_k - \xi_m)\right] = b_k, \quad k = 1, \dots, K \quad (14)$$

which can be again recast in the matrix form (10), where $\underline{b}$ is the sequence of the known terms, $\underline{x}$ is the sequence of the considered $\overline{q}$ unknown outside samples $F(\xi_m, \varphi)$, with $m = \overline{m}+1, \dots, \overline{m}+\overline{q}$, and $\underline{\underline{A}}$ is the $K \times \overline{q}$ matrix, whose elements are given by the weight functions in the considered CS expansion:

$$A_{km} = \operatorname{sinc}\left[\chi' W_\xi(\tilde{\xi}_k - \xi_m)\right] \quad (15)$$

Many numerical tests have been performed in order to compare the performances of both techniques. The reported results refer to a uniform planar circular array with radius equal to 20λ. Its elements, radially and azimuthally spaced of 0.8λ, are elementary Huygens sources linearly polarized along the y axis. Accordingly, an ellipsoidal source modelling with $2a = 40\lambda$ and $2b = 5\lambda$ has been used. The considered straight line is the radial line at $\varphi = 0°$ of a plane-polar domain located at distance $d = 12\lambda$ from the AUT center. The measurement interval is $[-35\lambda, 35\lambda]$. By choosing $\chi' = 1.15$ and an oversampling factor $\chi = 1.20$, the number of outside samples on each side is 5 for both sampling representations.

The following figures from 2 to 5 are reported for assessing the improvement achievable (without any extrapolation process) from the truncation error and stability viewpoints by employing the OSI expansions, instead of the CS ones. In particular, Figs. 2 and 3 confirm that, as already stated, a significant extension of the zone of good NF
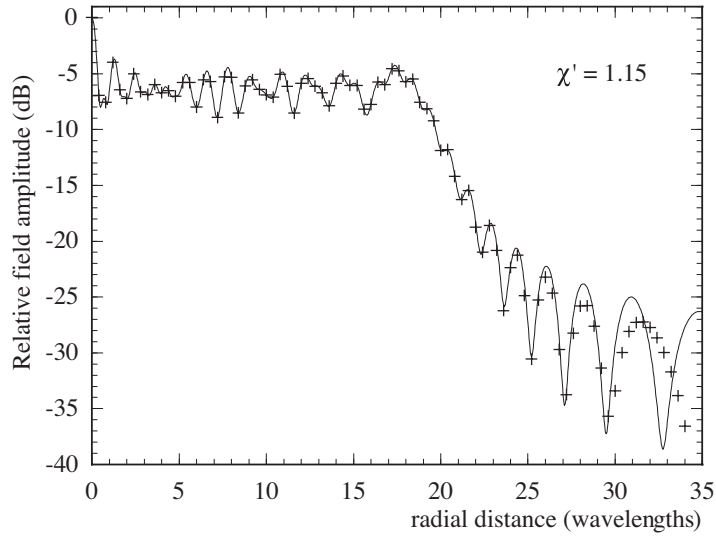
Figure 2. Amplitude of the NF y-component. Solid line: exact. Crosses: reconstructed via CS without estimated outside samples.
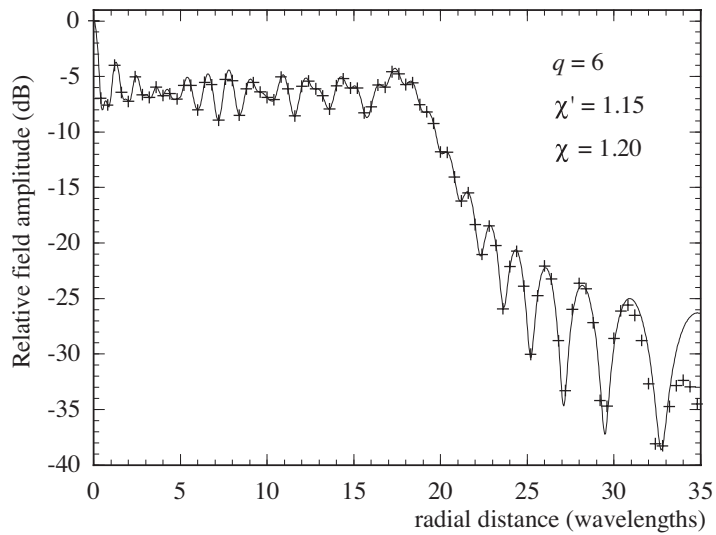
Figure 3. Amplitude of the NF y-component. Solid line: exact. Crosses: reconstructed via OSI without estimated outside samples.
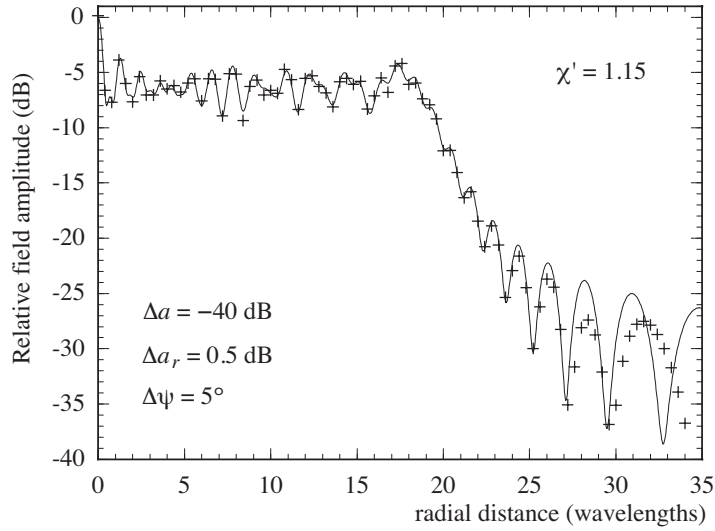
Figure 4. Amplitude of the NF y-component. Solid line: exact. Crosses: reconstructed via CS from error affected data without estimated outside samples.

reconstruction is attained when the OSI expansions are used. Whereas, Figs. 4 and 5 show that, in presence of errors affecting the data, a less accurate pattern recovery is obtained when using the CS ones. Both a background noise (bounded to Δa in amplitude and with arbitrary phase) and uncertainties on the data of $\pm\Delta a_r$ in amplitude and $\pm\Delta\psi$ in phase have been simulated by corrupting the ideal data by random errors.

Figure 6 highlights the improvement in the reconstruction accuracy achieved when using the CS based extrapolation procedure. The estimation has been performed by choosing $\overline{q} = 5$ and acquiring (on each side of the measurement interval) 7 extra samples at the middle points in between the regular sampling points starting from the end. Moreover, a truncated SVD (TSVD), which consists in zeroing the coefficients $1/\sigma_i$ corresponding to the small singular values σ_i of $\underline{\underline{A}}$, has been employed in order to improve the accuracy [25–27]. As can be seen, by taking into account the so estimated outside samples, the reconstruction is accurate not only in the whole measurement region, but also in a zone outside it.

Even better results are obtained if the OSI based extrapolation procedure is adopted (see Fig. 7). In such a case, $\overline{q}$ and the number of extra samples are the same of the CS based approach, but these last
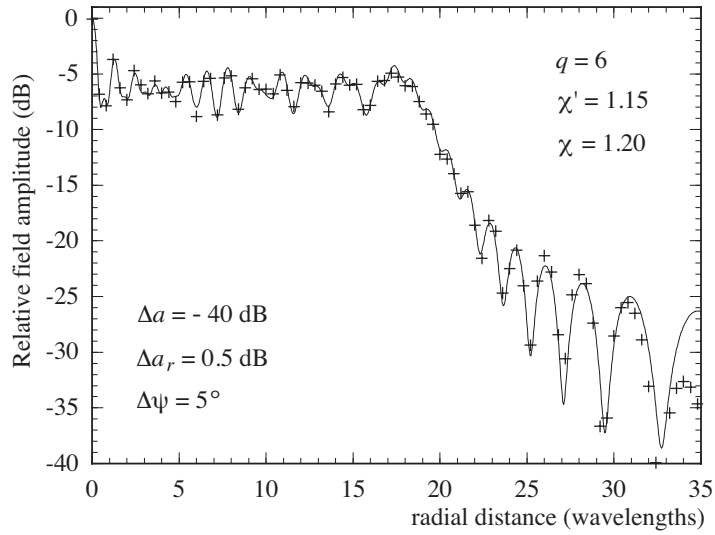
Figure 5. Amplitude of the NF y-component. Solid line: exact. Crosses: reconstructed via OSI from error affected data without estimated outside samples.
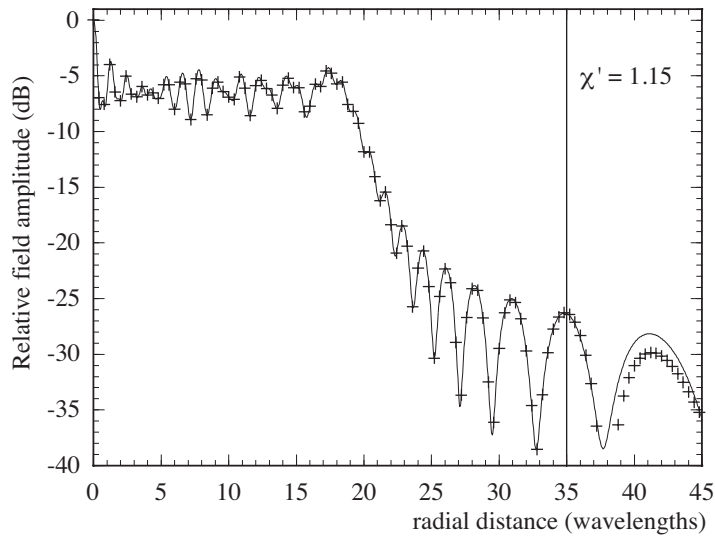
Figure 6. Amplitude of the NF y-component. Solid line: exact. Crosses: reconstructed via CS with outside samples estimated using TSVD.
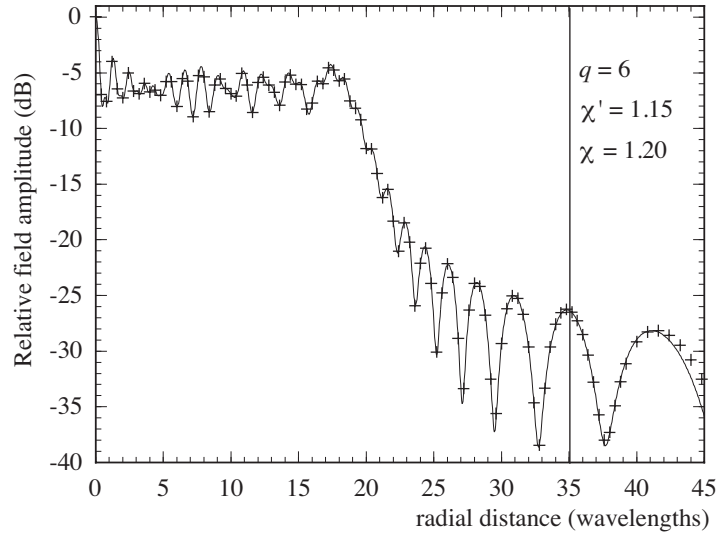
Figure 7. Amplitude of the NF y-component. Solid line: exact. Crosses: reconstructed via OSI with outside samples estimated using TSVD.

have been acquired at a 0.75λ step starting from the end. It is worthy to note that $q = 13$ has been used in (9), whereas $q = 6$ has been employed in the final interpolation.

Figures 8 and 9, which refer to error affected NF data, are analogous to the corresponding ones concerning exact NF samples (Figs. 6 and 7). Note that, in such a case, we have assumed $q = 9$ in the extrapolation process for reducing the propagation of errors from high to low field regions. As can be seen, also in presence of errors affecting the samples, the OSI based extrapolation procedure behaves better than the CS based one. Accordingly, only the former procedure will be employed in the following.

An alternative procedure to improve the accuracy of the solution achievable via the simple SVD is to adopt a Tikhonov regularization approach [28]. Such a solution corresponds to minimize the functional:

$$\left\| \underline{\underline{A}}\,\underline{x} - \underline{b} \right\|_2^2 + \alpha^2 \left\| \underline{x} \right\|_2^2 \tag{16}$$

α being the regularization parameter. Thus, the regularized solution $\underline{x}_{\mathrm{reg}}$ and the corresponding residual vector $\underline{b} - \underline{\underline{A}}\,\underline{x}_{\mathrm{reg}}$ can be written in
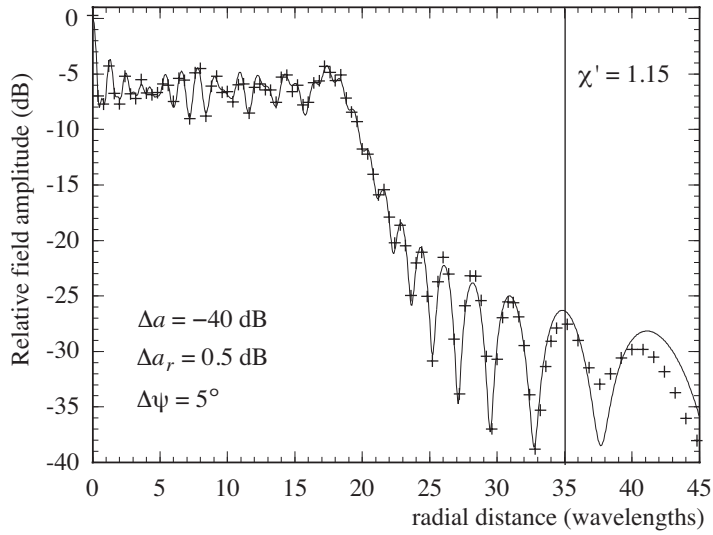
Figure 8. Amplitude of the NF y-component. Solid line: exact. Crosses: reconstructed via CS from error affected data with outside samples estimated using TSVD.
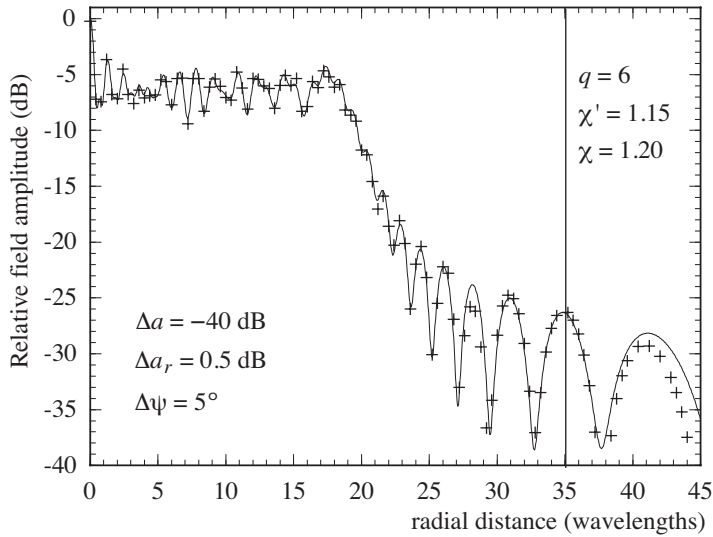
Figure 9. Amplitude of the NF y-component. Solid line: exact. Crosses: reconstructed via OSI from error affected data with outside samples estimated using TSVD.

term of the SVD of $\underline{\underline{A}}$ as

$$\underline{x}_{\text{reg}} = \sum_{i=1}^{\overline{q}} f_i \frac{\underline{u}_i^{\text{H}} \cdot \underline{b}}{\sigma_i} \underline{v}_i \tag{17}$$

$$\underline{b} - \underline{\underline{A}}\,\underline{x}_{\text{reg}} = \sum_{i=1}^{\overline{q}} (1 - f_i)\underline{u}_i^{\text{H}} \cdot \underline{b}\,\underline{u}_i + \sum_{i=\overline{q}+1}^{K} \underline{u}_i^{\text{H}} \cdot \underline{b}\,\underline{u}_i \tag{18}$$

In (17) and (18), the symbol H denotes the conjugate transposition operator, the singular values σ_i $(i = 1, \ldots, \overline{q})$ are ordered from the maximum to the minimum, $f_i = \sigma_i^2/(\sigma_i^2 + \alpha^2)$ are the corresponding filter factors, and $\underline{u}_i$, $\underline{v}_i$ are the left and right singular vectors of $\underline{\underline{A}}$, respectively [28]. The choice of the optimal parameter α to be used can be made by means of the L-curve [27], which is simply a plot of the norm of the regularized solution $\underline{x}_{\text{reg}}$ versus the corresponding residual norm of $\underline{b} - \underline{\underline{A}}\,\underline{x}_{\text{reg}}$ drawn in log-log scale for a set of admissible regularization parameters. In this way, the L-curve displays the compromise between the minimization of these two quantities, which is the heart of any regularization method. With reference to the Tikhonov regularization, the best compromise is represented by the so-called "corner", i.e., the distinct point separating the vertical and the horizontal parts of the curve.

Figures 10 and 11 refer to same cases considered in Figs. 7 and 9, but they have been obtained by using a Tikhonov regularization with the parameter α chosen via the L-curve. As can be seen, no particular gain results from the employ of this last regularization procedure in such a case.

3. ESTIMATION OF OUTSIDE DATA IN THE PLANE-POLAR SCANNING

In the first part of this section the key results relevant to the nonredundant NF-FF transformation with plane-polar scanning [4, 10] are briefly reported for reader's convenience.

These results rely on the extension of the aforementioned nonredundant representations of the EM fields to the voltage acquired by the probe. In fact, the voltage V measured by a non directive probe has the same effective (spatial) bandwidth of the field. The voltage representation from plane-polar data has been obtained [10] by describing the scanning plane by means of radial lines and rings, and assuming an oblate ellipsoid as surface Σ enclosing the AUT. In particular, the representation of the "reduced voltage" $\tilde{V}$ along a radial
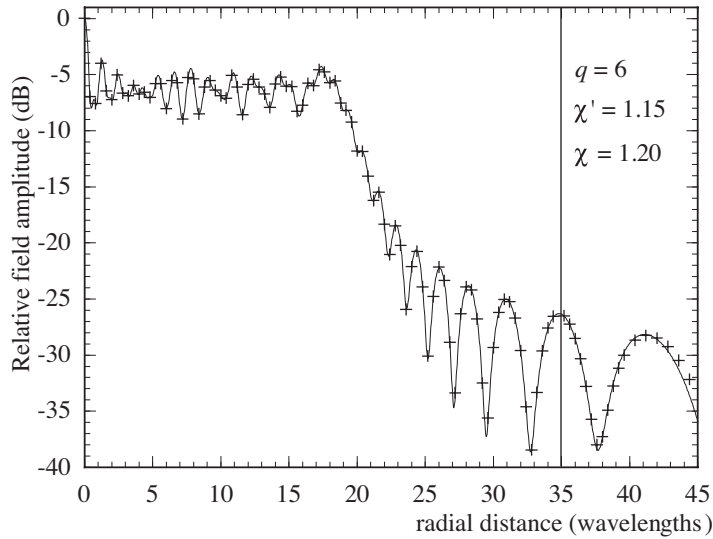
Figure 10. Amplitude of the NF *y*-component. Solid line: exact. Crosses: reconstructed via OSI with outside samples estimated using Tikhonov regularization.
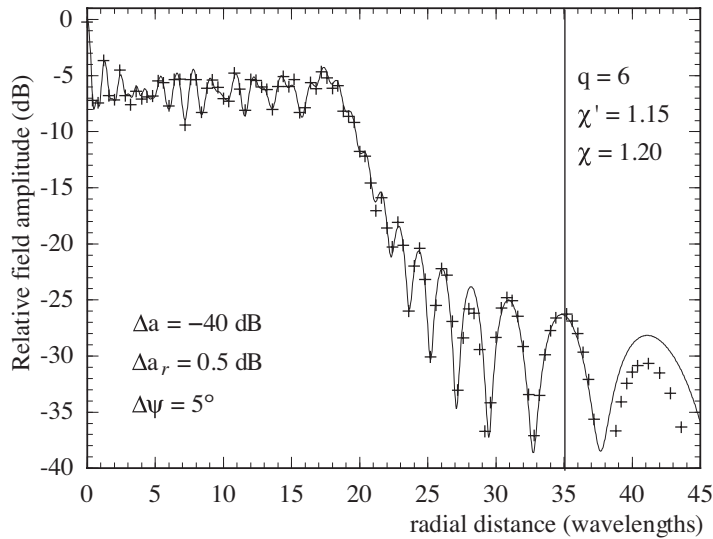
Figure 11. Amplitude of the NF *y*-component. Solid line: exact. Crosses: reconstructed via OSI from error affected data with outside samples estimated using Tikhonov regularization.

line is quite analogous to that (4) concerning the field, whereas, when considering a ring, the phase function is constant and it is convenient to use the azimuthal angle φ as optimal parameter. The corresponding bandwidth is $W_\varphi(\xi) = \beta a \sin \vartheta_\infty(\xi)$ [1, 4], $\vartheta_\infty = \sin^{-1} u$ being the polar angle of the asymptote to the hyperbola through the observation point. Accordingly, the proper OSI expansion along a ring at ξ_n is:

$$\tilde{V}(\xi_n, \varphi) = \sum_{m=m_0-p+1}^{m_0+p} \tilde{V}(\xi_n, \varphi_{m,n}) \Omega_{M_n}(\varphi - \varphi_{m,n}) D_{M_n''}(\varphi - \varphi_{m,n}) \quad (19)$$

wherein $m_0 = \text{Int}(\varphi/\Delta\varphi_n)$, $2p$ is the number of retained samples, and

$$\varphi_{m,n} = m\Delta\varphi_n = 2m\pi/(2M_n'' + 1); \quad M_n'' = \text{Int}(\chi M_n') + 1 \quad (20)$$
$$M_n' = \text{Int}(\chi^* W_{\varphi_n}) + 1; \quad M_n = M_n'' - M_n' \quad (21)$$
$$W_{\varphi_n} = W_\varphi(\xi_n); \quad \chi^*(\xi) = 1 + (\chi' - 1)[\sin \vartheta_\infty(\xi)]^{-2/3} \quad (22)$$

By properly matching the OSI expansions along ξ and along φ, we get:

$$\tilde{V}(\xi(\vartheta), \varphi) = \sum_{n=n_0-q+1}^{n_0+q} \left\{ \Omega_N(\xi - \xi_n) D_{N''}(\xi - \xi_n) \right.$$
$$\left. \cdot \sum_{m=m_0-p+1}^{m_0+p} \tilde{V}(\xi_n, \varphi_{m,n}) \Omega_{M_n}(\varphi - \varphi_{m,n}) D_{M_n''}(\varphi - \varphi_{m,n}) \right\}$$
$$(23)$$

Such an expansion can be employed to recover the NF data at each point of the measurement plane and, in particular, at the points required by the classical probe-compensated NF-FF transformation with plane-rectangular scanning [29]. In the here considered spherical reference system (R, Θ, Φ), the key relations for performing such a transformation are:

$$E_\Theta(\Theta, \Phi) = \left[I_H E'_{\Phi_V}(\Theta, -\Phi) - I_V E'_{\Phi_H}(\Theta, -\Phi) \right] / \Delta \quad (24)$$
$$E_\Phi(\Theta, \Phi) = \left[I_H E'_{\Theta_V}(\Theta, -\Phi) - I_V E'_{\Theta_H}(\Theta, -\Phi) \right] / \Delta \quad (25)$$

where E'_{Θ_V}, E'_{Φ_V} and E'_{Θ_H}, E'_{Φ_H} are the FF components radiated by the probe and the rotated probe when used as transmitting antennas,

$$\Delta = E'_{\Theta_H}(\Theta, -\Phi) E'_{\Phi_V}(\Theta, -\Phi) - E'_{\Theta_V}(\Theta, -\Phi) E'_{\Phi_H}(\Theta, -\Phi) \quad (26)$$

and

$$I_{V,H} = A\cos\Theta e^{j\beta d\cos\Theta}\int\limits_{-\infty}^{+\infty}\int\limits_{-\infty}^{+\infty}V_{V,H}(x,y)e^{j\beta x\sin\Theta\cos\Phi}e^{j\beta y\sin\Theta\sin\Phi}\mathrm{d}x\mathrm{d}y$$

(27)

A being a proper constant and I_V and I_H the two-dimensional Fourier transforms of the voltages V_V and V_H measured by the probe and the rotated probe, respectively.

Equations (24) and (25) are valid whenever the probe maintains its orientation with respect to the AUT and this requires that it rotates together with the AUT. Obviously, the positioning system is simplified when the probe co-rotation is avoided. Probes exhibiting only a first-order azimuthal dependence in their radiated far field (as, f.i., an open-ended cylindrical waveguide excited by a TE_{11} mode) can be used without co-rotation, since V_V and V_H can be evaluated from the knowledge of the measured voltages V_φ and V_ρ through the relations:

$$V_V = V_\varphi\cos\varphi - V_\rho\sin\varphi; \quad V_H = V_\varphi\sin\varphi + V_\rho\cos\varphi \quad (28)$$

Let us now tackle the problem of estimating the voltage samples external to the scanning region $\rho \leq \rho_{\max}$ in a plane-polar NF facility (see Fig. 12). If $\overline{n}$ is the index of the last ring inside such a zone,
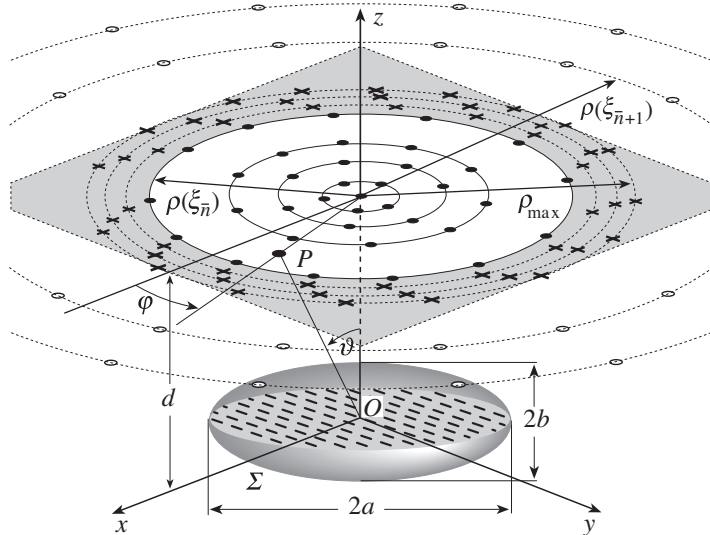
Figure 12. Relevant to the extrapolation of outside data in the plane-polar scanning.

let us assume the knowledge of the voltage data on the K rings at radii ρ_k, spaced at fixed step $\Delta\rho$ from $\rho_{\max}$, as in the one-dimensional case. On each of these rings, the samples are assumed known at the points specified by $\varphi_m = m\Delta\varphi_{\min}$, where $\Delta\varphi_{\min}$ is the azimuthal spacing between the samples to be estimated on the last considered outside ring. Moreover, it is convenient to estimate the same number of samples (at spacing $\Delta\varphi_{\min}$) on each outside ring. In such a way, the extra sampling points and the positions of samples on the external rings are all aligned, and the starting problem is reduced to an estimation procedure involving, each time, only a radial line. For each radial line, when reconstructing the reduced voltage at the extra sampling points, just $\overline{q} \leq q$ unknown outside samples are always involved in the OSI expansion along ξ, since the other q can be easily determined by applying (19). Accordingly, by assuming $\overline{n} + \overline{q} \leq n_0 + q$, we get the following overdetermined system:

$$\sum_{n=\overline{n}+1}^{\overline{n}+\overline{q}} \tilde{V}(\xi_n,\varphi_m)\Omega_N(\xi(\rho_k)-\xi_n)D_{N''}(\xi(\rho_k)-\xi_n) = \tilde{V}(\xi(\rho_k),\varphi_m) +$$

$$-\sum_{n=n_0-q+1}^{\overline{n}} \tilde{V}(\xi_n,\varphi_m)\Omega_N(\xi(\rho_k)-\xi_n)D_{N''}(\xi(\rho_k)-\xi_n) = b_k, \ \ k=1,\ldots,K$$

$$(29)$$

Also in such a case, the above linear system can be rewritten in the matrix form (10) and solved via SVD.

It is worthy to note that, on each extra ring, it is convenient to collect the samples in the positions fixed by the nonredundant sampling representation and to reconstruct the data needed at $\Delta\varphi_{\min}$ spacing via the OSI expansion (19), thus minimizing the number of extra samples to be acquired.

Numerical tests assessing the effectiveness of the approach are reported in the following. The simulation refers to the same AUT and scanning plane considered in the previous section. An open-ended cylindrical waveguide with radius $a' = 0.338\lambda$ is chosen as probe, thus allowing to avoid the probe co-rotation.

As in the one-dimensional case, the radii of the extra rings are spaced at fixed step $\Delta\rho = 0.75\lambda$ from $\rho_{\max}$. It is worthy to note that the number of rings needed to cover the range $]35\lambda, +\infty[$ is 5. In the reported example, we have considered $\overline{q} = 5$, $K = 7$ and have assumed $q = 13$ in the extrapolation process, whereas $p = 8$ has been adopted in (19) to obtain the involved known samples. It must be stressed that the SVD is applied to a small matrix with a negligible computational effort.
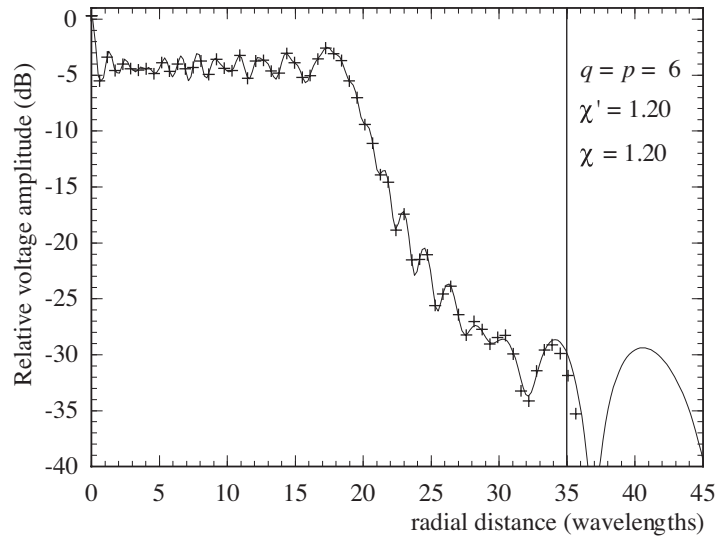
Figure 13. Amplitude of V_V on the radial line at $\varphi = 90°$. Solid line: exact. Crosses: reconstructed without estimated outside samples.

Figure 13 shows the amplitude of the voltage V_V (the most significant one) on the radial line at $\varphi = 90°$. It has been reconstructed without using the extrapolation process and putting the outside samples equal to zero. The result is not good in the range where the knowledge of the outside samples is needed. As can be seen in Fig. 14, by using the described estimation procedure, the reconstruction is very accurate not only in the whole measurement region, but also in an extended zone outside it. It is worthy to note that, in both cases, $p = q = 6$ have been adopted when applying (23) for the final voltage reconstruction. Analogous comments can be made for Figs. 15 and 16, which are relevant to the reconstruction on the radial line at $\varphi = 60°$.

To assess the effectiveness of the approach in a more quantitative way, the maximum and mean-square reconstruction errors have been evaluated by comparing in the measurement zone the exact voltage values and those reconstructed with and without the estimated outside samples. Figure 17 shows such errors, normalized to the voltage maximum value on the plane, for $\chi = \chi' = 1.20$, and some $p = q$ values. As can be seen, the errors evaluated by taking into account the estimated samples decrease until very low levels are reached. On the contrary, those obtained without considering them saturate to constant values, due to the truncation error present near to the boundary of the measurement region.
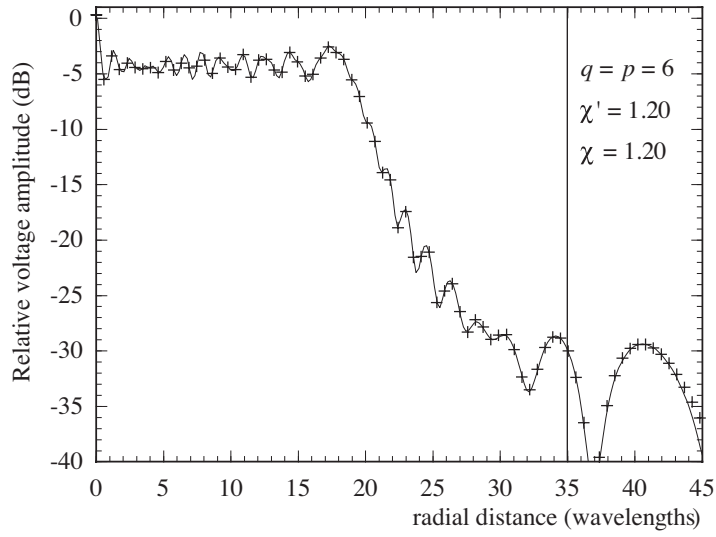
Figure 14. Amplitude of V_V on the radial line at $\varphi = 90°$. Solid line: exact. Crosses: reconstructed with estimated outside samples.
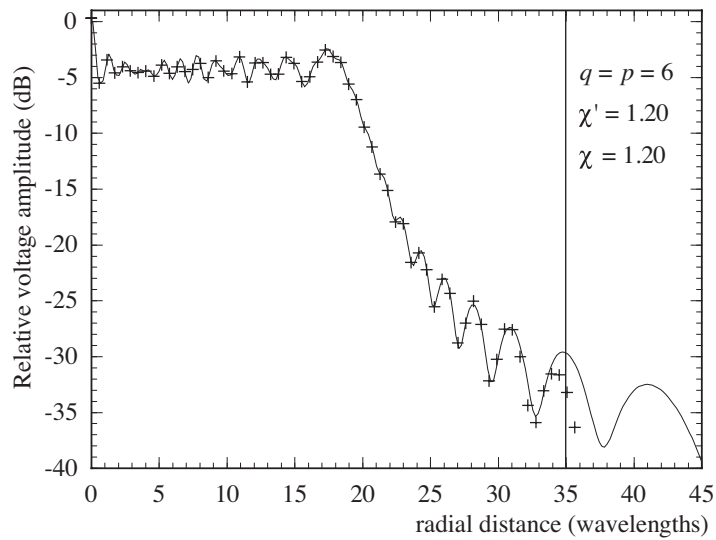
Figure 15. Amplitude of V_V on the radial line at $\varphi = 60°$. Solid line: exact. Crosses: reconstructed without estimated outside samples.
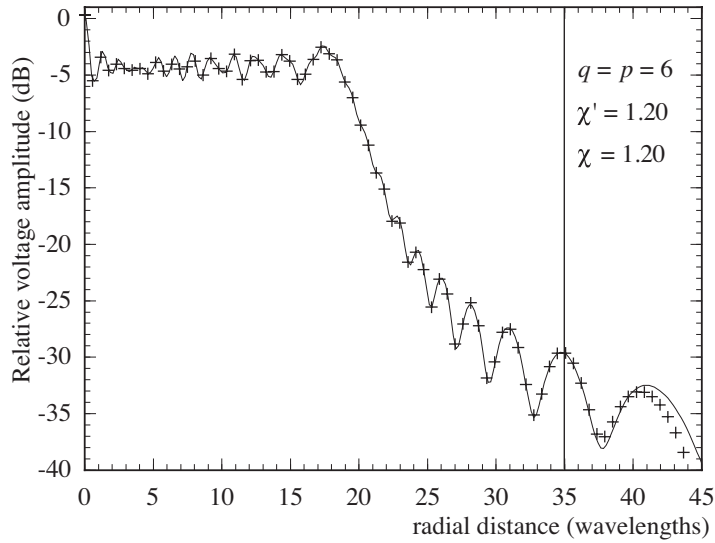
Figure 16. Amplitude of V_V on the radial line at $\varphi = 60°$. Solid line: exact. Crosses: reconstructed with estimated outside samples.
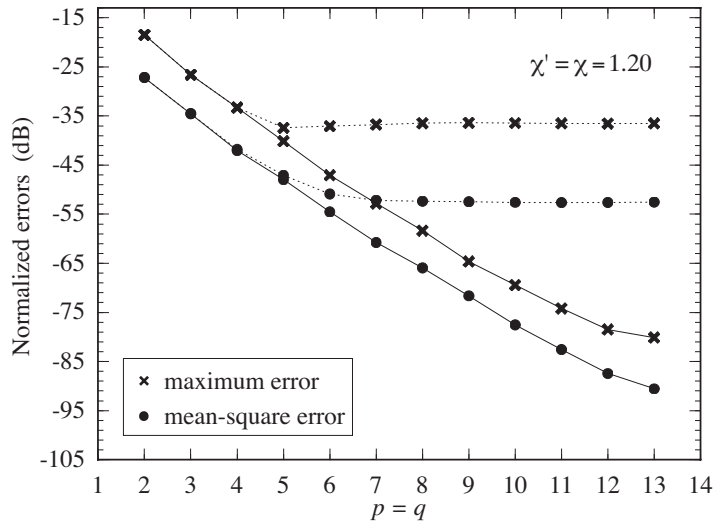
Figure 17. Reconstruction errors of V_V. Dashed lines: without estimated outside samples. Solid lines: with estimated outside samples.
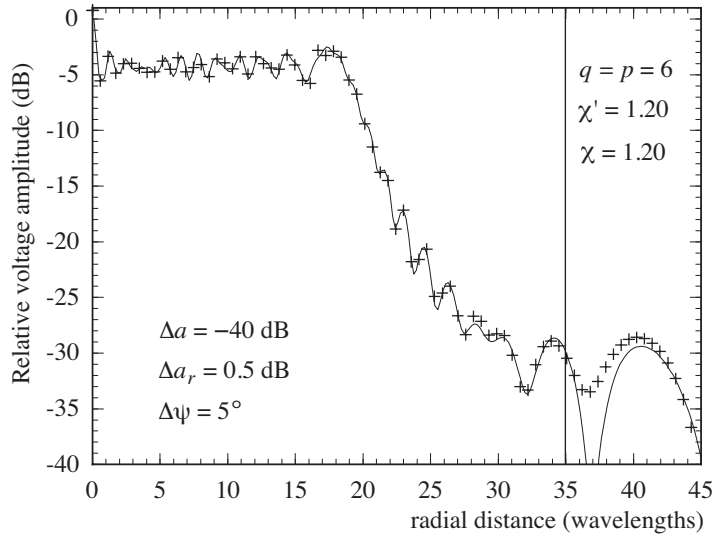
Figure 18. Amplitude of V_V on the radial line at $\varphi = 90°$. Solid line: exact. Crosses: reconstructed from error affected data with estimated outside samples.

The stability of the algorithm has been investigated by adding random errors to the exact samples. These errors simulate a background noise (bounded to Δa in amplitude and with arbitrary phase) and uncertainties on the data of $\pm\Delta a_r$ in amplitude and $\pm\Delta\psi$ in phase. As shown in Fig. 18, the technique works well also in presence of errors.

The described technique has been applied to recover the plane-rectangular data needed for the probe compensated NF-FF transformation and lying in a $100\lambda \times 100\lambda$ square grid. Figures 19 and 20 report the AUT pattern in the E-plane, reconstructed via the NF-FF transformation without and with estimated outside samples, respectively.

As can be seen, the FF reconstruction obtained by considering the estimated samples is accurate in a significantly wider angular range. In fact, as can be seen in Figs. 19 and 20, the angular extension of the good FF reconstruction zone increases about 35% for the considered example.

It is useful to note that the number of employed NF data in the reported example is 12 151 significantly less than those (30 731) needed by the NF-FF transformation [30]. In particular, the number of extra samples is 2 355.
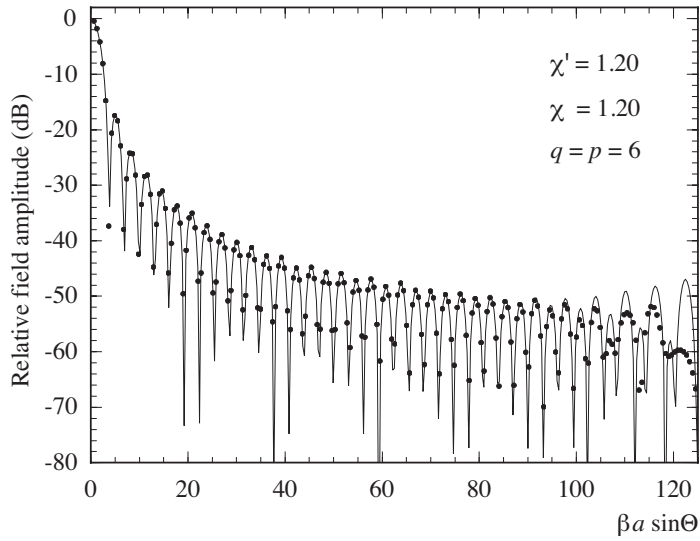
Figure 19. FF pattern in the *E*-plane. Solid line: exact field. Dots: reconstructed from NF data without estimated outside samples.
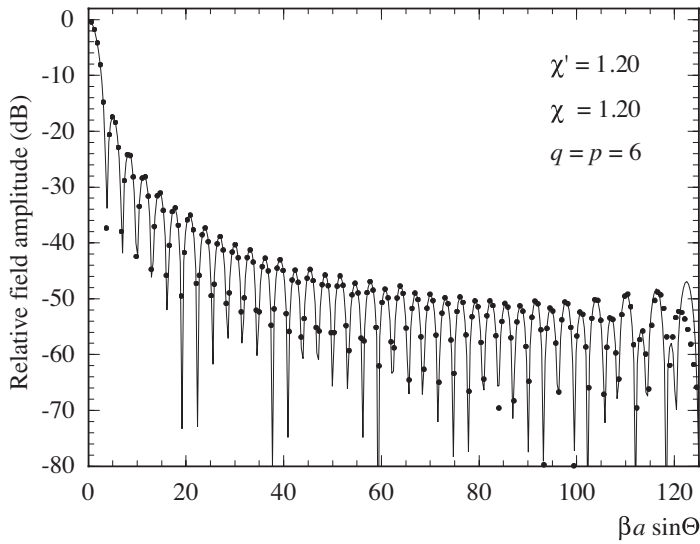
Figure 20. FF pattern in the *E*-plane. Solid line: exact field. Dots: reconstructed from NF data with estimated outside samples.

4. CONCLUSION

In this paper, we have proposed an effective technique for extrapolating the NF data external to the measurement region in the plane-polar scanning. It allows a significant reduction of the error related to the truncation of the scan zone. Such a technique relies on the nonredundant sampling representations of the EM fields and on the OSI expansions of central type, and uses the SVD method for estimating the outside samples. The comparison of this approach with a procedure available in literature and employing the CS expansions has shown that the proposed technique works better. Numerical simulations assessing the effectiveness of the extrapolation procedure are reported. In particular, they show that a significant enlargement of the good FF reconstruction zone is attainable when considering the so estimated data.

REFERENCES

1. Bucci, O. M., C. Gennarelli, and C. Savarese, "Representation of electromagnetic fields over arbitrary surfaces by a finite and nonredundant number of samples," *IEEE Trans. Antennas Propagat.*, Vol. 46, 351–359, 1998.
2. Bucci, O. M. and G. Franceschetti, "On the spatial bandwidth of scattered fields," *IEEE Trans. Antennas Propagat.*, Vol. AP-35, 1445–1455, 1987.
3. Bucci, O. M., C. Gennarelli, G. Riccio, and C. Savarese, "Near-field-far-field transformation from nonredundant plane-polar data: effective modellings of the source," *IEE Proc. - Microw., Antennas Propagat.*, Vol. 145, 33–38, 1998.
4. Bucci, O. M., F. D'Agostino, C. Gennarelli, G. Riccio, and C. Savarese, "NF-FF transformation with plane-polar scanning: ellipsoidal modelling of the antenna," *Automatika*, Vol. 41, 159–164, 2000.
5. D'Agostino, F., C. Gennarelli, G. Riccio, and C. Savarese, "Data reduction in the NF-FF transformation with bi-polar scanning," *Microw. Opt. Technol. Lett.*, Vol. 36, 32–36, 2003.
6. Ferrara, F., C. Gennarelli, R. Guerriero, G. Riccio, and C. Savarese, "An efficient near-field to far-field transformation using the planar wide-mesh scanning," *J. Electromagn. Waves Appl.*, Vol. 21, 341–357, 2007.
7. D'Agostino, F., F. Ferrara, C. Gennarelli, G. Riccio, and C. Savarese, "NF-FF transformation with cylindrical scanning

from a minimum number of data," *Microw. Opt. Technol. Lett.*, Vol. 35, 264–270, 2002.

8. Bucci, O. M., F. D'Agostino, C. Gennarelli, G. Riccio, and C. Savarese, "Data reduction in the NF-FF transformation technique with spherical scanning," *J. Electromagn. Waves Appl.*, Vol. 15, 755–775, 2001.

9. D'Agostino, F., C. Gennarelli, G. Riccio, and C. Savarese, "Theoretical foundations of near-field-far-field transformations with spiral scannings," *Progress In Electromagnetics Research*, PIER 61, 193–214, 2006.

10. Gennarelli, C., G. Riccio, F. D'Agostino, and F. Ferrara, *Near-field - Far-field Transformation Techniques*, Vol. 1, CUES, Salerno, Italy, 2004.

11. Bucci, O. M., C. Gennarelli, and C. Savarese, "Optimal interpolation of radiated fields over a sphere," *IEEE Trans. Antennas Propagat.*, Vol. AP-39, 1633–1643, 1991.

12. Slepian, D. and H. O. Pollak, "Prolate spheroidal wave functions, Fourier analysis and uncertainty — I," *Bell Syst. Tech. J.*, Vol. 40, 43–63, 1961.

13. Papoulis, A., "A new algorithm in spectral analysis and band-limited extrapolation," *IEEE Trans. Circuits, Syst.*, Vol. CAS-22, 735–742, 1975.

14. Sabri, M. S. and W. Steenaart, "An approach to band-limited signal extrapolation: the extrapolation matrix," *IEEE Trans. Circuits, Syst.*, Vol. CAS-25, 74–78, 1978.

15. Cadzow, J. A., "An extrapolation procedure for band-limited signals," *IEEE Trans. Acoust., Speech, Signal Processing*, Vol. ASSP-27, 4–12, 1979.

16. Jain, A. K. and S. Ranganath, "Extrapolation algoritms for discrete signals with application in spectral estimation," *IEEE Trans. Acoust., Speech, Signal Processing*, Vol. ASSP-29, 830–845, 1981.

17. Sanz, J. L. C. and T. S. Huang, "Some aspects of band-limited signal extrapolation: models, discrete approximation, and noise," *IEEE Trans. Acoust., Speech, Signal Processing*, Vol. ASSP-31, 830–845, 1983.

18. Sullivan, B. J. and B. Liu, "On the use of singular value decomposition and decimation in discrete-time band-limited signal extrapolation," *IEEE Trans. Acoust., Speech, Signal Processing*, Vol. ASSP-32, 1201–1212, 1994.

19. Sano, A., "Optimally regularized inverse of singular value decomposition and application to signal extrapolation," *Signal Processing*, Vol. 30, 163–176, 1993.

20. Ferreira, P. J. S. G., "The stability of a procedure for the recovery of lost samples in band-limited signals," *Signal Processing*, Vol. 40, 195–205, 1994.

21. Landau, H. J., "Extrapolating a band-limited function from its samples taken in a finite interval," *IEEE Trans. Inf. Theory*, Vol. IT-32, 464–470, 1986.

22. Bucci, O. M., G. D'Elia, and M. D. Migliore, "A new strategy to reduce the truncation error in near-field/far-field transformations," *Radio Science*, Vol. 35, 3–17, 2000.

23. Bucci, O. M., G. D'Elia, and M. D. Migliore, "Experimental validation of a new technique to reduce the truncation error in near-field far-field transformation," *Proc. of AMTA 1998*, 180–185, Montreal, Canada, 1998.

24. Bolomey, J. C., O. M. Bucci, L. Casavola, G. D'Elia, M. D. Migliore, and A. Ziyyat, "Reduction of truncation error in near-field measurement of antennas of base-station mobile communication systems," *IEEE Trans. Antennas Propagat.*, Vol. 52, 593–602, 2004.

25. Golub, G. H. and C. F. Van Loan, *Matrix Computations*, John Hopkins University Press, Baltimore, 1996.

26. Press, W. H., S. A. Teukolsky, W. T. Vetterling, and B. P. Flannery, *Numerical Recipes*, Cambridge University Press, New York, 1999.

27. Hansen, P. C., *Rank-deficient and Discrete Ill-posed Problems*, SIAM, Philadelphia, USA, 1998.

28. Tikhonov, A. N. and V. Y. Arsenin, *Solutions of Ill-posed Problems*, Winston, Washington, D.C., USA, 1977.

29. Paris, D. T., W. M. Leach, Jr., and E. B. Joy, "Basic theory of probe-compensated near-field measurements," *IEEE Trans. Antennas Propagat.*, Vol. AP-26, 373–379, 1978.

30. Gatti, M. S. and Y. Rahmat-Samii, "FFT applications to plane-polar near-field antenna measurements," *IEEE Trans. Antennas Propagat.*, Vol. AP-36, 781–791, 1988.